Phase diffusion in a chaotic pendulum

James A. Blackburn
Department of Physics and Computing, Wilfrid Laurier University, Waterloo, Ontario, Canada

Niels Grønbech-Jensen
Theoretical Division, Los Alamos National Laboratory, Los Alamos, New Mexico

(Received 17 August 1995)

The rate of expansion of the phase coordinate for a harmonically driven pendulum is considered. The mean-squared displacement is found to grow as a linear function of time during chaotic motion, indicating deterministic diffusion. The diffusion coefficient can be significantly influenced by the proximity of a window containing a periodic solution. We find that diffusion associated with intermittent chaos can be described in terms of an interleaving of the diffusion properties of the separate modes taking part in the intermittency.

PACS number(s): 05.45.+b, 74.40.+k

INTRODUCTION

The simple pendulum with velocity-dependent damping and harmonic forcing has emerged as one of a select group of model systems commonly employed in the investigation of chaotic dynamics [1]. Motion of the pendulum mass about the pivot can be viewed as an evolving trajectory in the phase plane $(\theta,\dot{\theta})$. When the physical parameters of the system are chosen so as to result in chaotic behavior, the long-time evolution of the phase space coordinate θ may exhibit expansion properties characteristic of classical diffusion—a mean-squared amplitude that depends linearly on time. Such deterministic diffusion is of course intimately tied to the nature of the chaotic state from which it emerges —the process is not propelled by any stochastic forces. The particulars of this behavior are the issues of interest here.

Publications on the topic of chaos-induced diffusion have appeared mainly within the past decade. Most of this work has been based on the climbing-sine map $x_{t+1}=x_t-\mu\sin(2\pi x_t)$ [2–5], although circle maps [6], logistic maps [7], and piecewise linear maps [8,9] were also employed. Geisel *et al.* [10] analyzed the motion of a particle in a two-dimensional "egg carton" potential, finding diffusive behavior.

Deviations from linearity, such that the mean squared displacement is proportional to t^{γ} with $\gamma\neq 1$, are hallmarks of what is termed anomalous diffusion. The relationship between anomalous deterministic diffusion and intermittent chaos has been explored recently by a number of authors [11–18] who have mostly focused on iterated maps.

While it may be convenient and even appealing to utilize circle maps, sine maps, logistic maps, etc., as starting points in the theoretical attack on various problems in chaos, nevertheless the nonlinear physical world remains essentially continuous in time and somewhat more complex, albeit some two-dimensional maps have been demonstrated to model analogs of three-dimensional time continuous systems [19]. In the spirit of returning to these realities, we consider here the manifestation of deterministic diffusion in a driven pendulum. This investigation derives additional motivation from the well known isomorphism of the driven pendulum to current biased Josephson junctions [20–22].

THEORY

A pendulum is taken to consist of a mass m located at a distance ℓ from a pivot and oriented at an angle θ with respect to the vertical. The total moment of inertia of the complete system, produced by m together with any other corotating components, is I. Let b be the coefficient of velocity-dependent friction. Then the equation of motion is

$$I\frac{d^2\theta}{dt^2}+b\frac{d\theta}{dt}+mg\ell\sin(\theta)=\Gamma\sin(\omega t), \tag{1}$$

where Γ and ω are the amplitude and frequency of the applied ac torque. It is conventional practice to normalize time to units of the reciprocal of the small amplitude natural frequency $\omega_0=\sqrt{mg\ell/I}$, employing overdots to signify dimensionless time derivatives, and to express torque in units of $mg\ell$. Then (1) becomes

$$\ddot{\theta}+\left[\frac{1}{Q}\right]\dot{\theta}+\sin(\theta)=\epsilon\sin(\Omega\tau), \tag{2}$$

from which it is clear that there are in reality only three independent (dimensionless) defining parameters for the driven pendulum: they are $Q=\sqrt{mg\ell I}/b$, $\epsilon=\Gamma/(mg\ell)$, and $\Omega=\omega/\omega_0$.

It is well known [1,21–25] that chaotic motion for the pendulum is easily achieved and that the zones of chaos in the three-dimensional state space (Q,ϵ,Ω) form rather complex structures. In point of fact, the very extent of this intricately divided state space creates practical problems for any study of particular aspects of chaos in this system. That is, where should the investigation be localized? For this study, we settled on drive parameter values, $\epsilon=0.78$ and $\Omega=0.62$, although the results to be discussed are not in any fundamental way tied to these exact numbers, and simulations with other values revealed qualitatively similar behavior. The normalized damping parameter Q was then allowed to vary over the range $3.0\leqslant Q\leqslant 7.0$ This placed the operating point somewhere near the lower region of Octavio's Fig. 4 [22], observing that in his notation $\beta_C=Q^2$, $\rho=\epsilon$, and

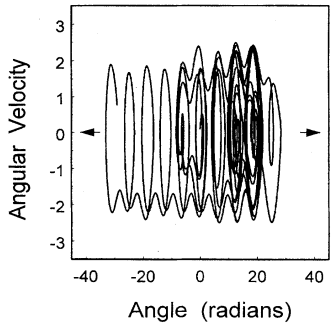

FIG. 1. Phase plane orbit for a chaotic state with $\epsilon=0.78, \Omega=0.62$, and $Q=5.14$. As time proceeds, the outer limits of the orbit expand to the left and right, as suggested by the arrows. Angular velocity is measured in radians per dimensionless time unit.

$\Omega=0.65$. This also situated the operating point near the lower portion of the state diagram shown as Fig. 12 in Blackburn *et al.* [23].

Numerical solutions of (2) were obtained using a fourth-order Runge-Kutta algorithm with nominal fixed step size set at 1% of the drive period. This time step was found to be sufficiently small when simulating continuous time properties of the system. Simulations with half this time step resulted in identical statistical behavior of Lyapunov exponents and diffusion constants, which we will discuss in the following sections. Here it is important to notice that due to the inherent nature of chaos, only statistical properties can be expected to compare well when the time step is changed.

DETERMINISTIC DIFFUSION

The general appearance of a typical chaotic phase plane orbit is illustrated in Fig. 1, where the arrows indicate that, over time, the trajectory is expanding outwards to the left and right. Figure 2 presents a pair of time series of the square of the pendulum angle $[\theta(\tau)]^2$, each obtained as solutions to (2) for nearly (but not quite) identical initial conditions chosen close to the origin in the phase plane. It is immediately apparent that (a) the two curves are radically different

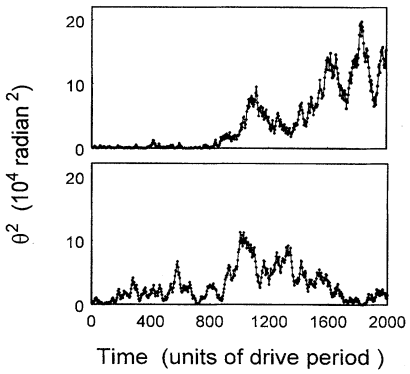

FIG. 2. Typical time series $\theta^2(\tau)$ for $Q=4.00$ computed from almost identical initial conditions.

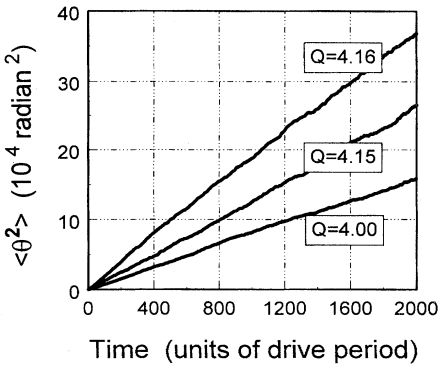

FIG. 3. Ensemble averages $\langle[\theta(\tau)]^2\rangle$ for three different values of damping coefficient Q. The linearity of these plots indicates deterministic diffusion.

from one another and (b) individually they are clearly not monotonic in time.

In Fig. 3, *ensemble averages* $\langle[\theta(\tau)]^2\rangle$ are plotted, where the averaging $\langle\rangle$ was taken over a 40×40 grid of initial conditions centered around the origin $\theta=0, \dot{\theta}=0$. That is, 1600 individual time series such as are shown in Fig. 2 are summed. Each series spanned a total elapsed time of 2000 drive periods, and there were 100 integration steps per drive cycle. Thus a total of 320×10^6 Runge-Kutta iterations are executed for every fixed Q line in Fig. 3. The contrast between single time series as in Fig. 2 and the ensemble averages as in Fig. 3 is, however much anticipated, remarkable. The slopes of these essentially linear characteristics yield diffusion coefficients, or more precisely, $\frac{1}{2}(slope)=D$. Plots of very similar appearance, but obtained for 2000 starting points of a sine map, are to be found in Fig. 1 of Geisel and Nierwetberg [3].

The results to this point establish that the driven pendulum does indeed exhibit phase diffusion during chaotic motion. However, the choice of dissipation constant Q has so far been arbitrary in the sense that certain values have been selected that certainly lead to the phenomenon of interest, but no systematic role for Q has been explored; this we now undertake.

As a necessary first step, a bifurcation diagram was computed for a range of dissipation coefficients between 3.0 and 7.0, these being deemed to be physically sensible values. Data were generated by sampling the evolving numerical solution of (2) once per drive cycle (Poincaré section) for a total duration of 1000 drive cycles. This was done for each of 200 Q values within the indicated range. The bifurcation diagram shown in Fig. 4 reveals a not-unexpected richness of detail, involving many periodic windows embedded within the prevalent chaos. The dissipation coefficients Q=4.00, 4.15, and 4.16 chosen for the previous figure can be seen to lie just inside the chaotic zone that precedes the largest periodic window.

It was quickly evident from simulation data that diffusion coefficients of similar magnitudes could be found for chaotic states over the entire range of dissipation constants used in Fig. 4. In other words, D is certainly not any simple function of Q. However, it was also apparent that the diffusion rate could be considerably enhanced very close to the edge of a

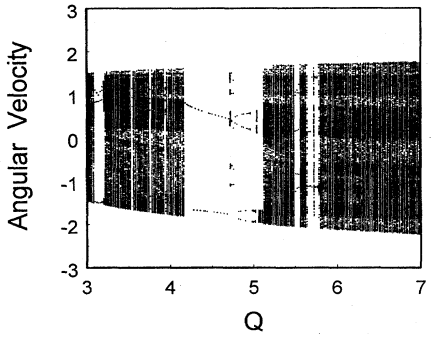

FIG. 4. A bifurcation diagram for the driven pendulum with $\epsilon=0.78$ and $\Omega=0.62$. Angular velocity is measured in radians per dimensionless time unit.

periodic window. Two particular windows were selected for closer examination: W_A, [3.085,3.212]; and W_B, [4.175, 5.110]. W_A contains closed period-3 orbits; W_B contains running period-1 solutions.

From the slopes of plots of $\langle[\theta(\tau)]^2\rangle$ versus τ, diffusion coefficients were determined at a number of selected Q values on either side of the two periodic windows. These are displayed in Fig. 5. The most straightforward interpretation of the general features in this graph is that the chaotic solution begins to "anticipate" the periodic state as the window edge is approached, and consequently the diffusion coefficient D alters accordingly near a window boundary.

Nonrunning periodic orbits do not expand in phase space—they form closed curves that repeat themselves—and so must have an associated diffusion coefficient $D=0$. This is the case within window W_A. As can be seen in the figure, D remains quite small just outside the domain of W_A.

In contrast, window W_B consists of running solutions that certainly do expand in phase space, but not in a diffusive manner. The period-1 orbits are synchronized to the ac forcing term and so each advance of 2π occurs in one drive period. Neglecting undulations, an approximate expression for this motion is $\theta\approx\Omega\tau$ where τ is dimensionless time

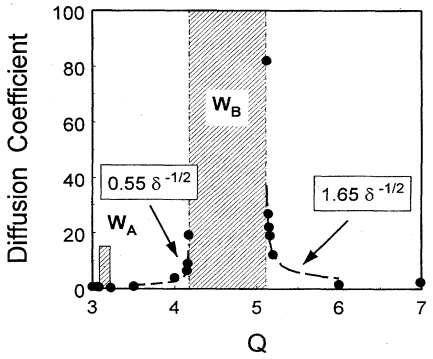

FIG. 5. Diffusion coefficients (solid dots) determined from slopes of $\langle\theta^2\rangle$ versus τ plots at selected Q values. The units of D are radians^2 per drive period. The shaded regions are the periodic windows referred to in the text. The parameter δ is defined as $|Q-Q_C|$where Q_C is a window boundary.

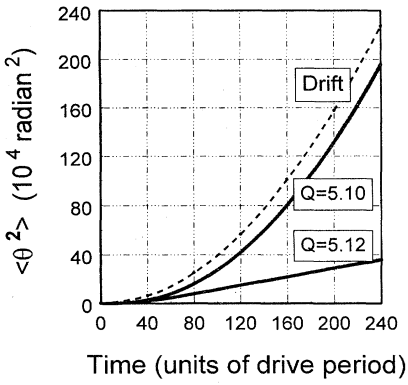

FIG. 6. Ensemble averages $\langle[\theta(\tau)]^2\rangle$ for values of the dissipation constant immediately on either side of the window boundary at $Q_C=5.110$. The dotted line is the limiting form for drift motion of the phase coordinate.

as before and, for this study, $\Omega=0.62$. Thus $\langle\theta^2\rangle=(0.3844)\tau^2$ describes the limiting form of phase expansion associated with running periodic orbits in window W_B. This quadratic dependence of the mean squared displacement on time is fundamentally different from the linear relationship associated with diffusion, and is instead the result of *phase drift*. This is illustrated in Fig. 6, where $\langle\theta^2\rangle$ versus τ is displayed for Q values lying immediately on either side of the window boundary at $Q_C=5.110$. The dotted line is the pure drift curve.

Schell *et al.* [2] considered deterministic diffusion for the climbing-sine map and concluded that "near bifurcation the diffusion coefficient depends on the square root of the deviation of the map parameter from bifurcation." For transitions to running solutions they found the functional form (in our notation) to be $|Q-Q_C|^{-1/2}$, and for transitions to periodic solutions, the diffusion coefficient varied as $|Q-Q_C|^{+1/2}$, where Q_C denotes a boundary value of the dissipation constant. Our data for the driven pendulum are consistent with these expressions, and the inverse square root dependence is particularly convincing immediately on either side of window W_B, as is evident in Fig. 5.

Well away from window boundaries, the diffusion coefficient subsides to comparatively small values. It is tempting to take the comment by Chaudhuri *et al.* [26], "...the Lyapunov exponent is a measure of rate of divergence of initially nearby trajectories, as a consequence of which the diffusive motion in phase space takes place," and seek an explicit connection between the Lyapunov coefficient λ and the diffusion constant D. However, consider Fig. 7, which is a plot of computed Lyapunov coefficients versus dissipation constant for window W_A. The region $3.186\leq Q\leq 3.212$ has positive λ, is associated with nonrotating chaotic period-3 orbits, and does not exhibit deterministic diffusion. In fact, $D=0$ throughout the window, while λ ranges extensively from negative to positive values, suggesting that no direct relationship between λ and D is possible in general. Similarly, we have found large windows of nearly constant λ for which the diffusion constant varies dramatically. We note parenthetically the interesting strong similarity of Fig. 7 here to Fig. 11 in Kautz and Macfarlane [21] in which purely peri-

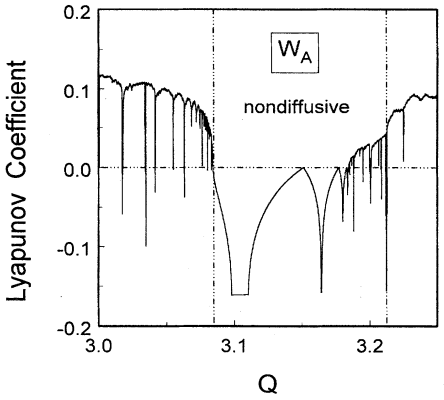

FIG. 7. Lyapunov coefficient versus dissipation constant over a region bracketing the period-3 window.

odic ($\lambda<0$) states for an rf driven Josephson junction precede locked-chaotic ($\lambda>0$) ones, before full chaos is reached.

INTERRUPTED DIFFUSION

As noted in the Introduction, recent work on iterated maps [4,13] has suggested that a new behavior (anomalous diffusion) appears during intermittent chaos. As a means of investigating this issue with respect to the driven pendulum, we first located an intermittent mode at $Q=5.78$. This state is characterized as having a pair of coexisting antisymmetric nonrotating period-2 orbits. Numerical simulations revealed that the system switches back and forth between these periodic modes at irregular intervals, and that it is chaotic during the transition phase. Such behavior is evident in the plot of Fig. 8, where the horizontal plateaus result from one or the other periodic motion. Brief chaotic bursts signal the transitions.

The Poincaré section for $Q=5.78$ is shown in Fig. 9; it was generated from a numerical simulation extending over 40 000 drive cycles, with one sampled point taken per drive cycle. Any period-2 state manifests itself in a Poincaré section as a *pair* of points or line segments that share "hits" on alternate drive cycles; accordingly the boxed segments in the figure are linked in pairs to signify each attractor. There are

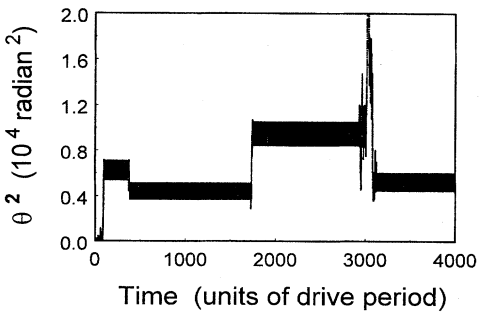

FIG. 8. Typical time series $\theta^2(\tau)$ for the intermittent case $Q=5.78$. The system is periodic during horizontal plateaus, and chaotic during transitional bursts.

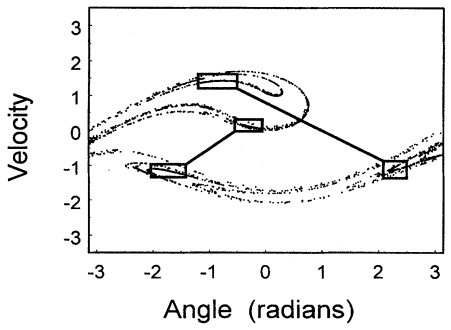

FIG. 9. Poincaré section for $Q=5.78$. The linked boxes indicate the locations of accumulation segments for each of the period-2 orbits on the attractor. Angular velocity is measured in radians per dimensionless time unit.

then three constituent parts to this figure—short segments (enclosed in boxes) associated with each of the two periodic modes, and the much more extensive chaotic strange attractor.

In like fashion to the procedures associated with Fig. 3, ensemble averages $\langle[\theta(\tau)]^2\rangle$ were computed for the intermittent case $Q=5.78$, as well as for the purely chaotic case $Q=5.79$. The results are plotted in Fig. 10. It is quite apparent that the rate of expansion of the mean-squared amplitude changes from that of a chaotic state at small time to a much lower value above $\tau\approx200$. The behavior at small time is in fact only an artifact of the initial conditions employed in the individual simulation runs comprising the complete ensemble total of 1600. The initial conditions were selected from a cluster centered around the origin in the phase plane. This choice always started the system in chaos from which it inevitably moved to intermittency. In the ensemble averaging the first-chaos behavior leads to a preliminary rapid diffusion, as the figure indicates. However, after this early effect has passed, a much lower slope in the mean-squared displacement is evident. Furthermore, we have verified by modifying the initial condition selection process that this early effect can be eliminated entirely, with a linear expansion occurring all the way to the origin. From the slopes in Fig. 10 we conclude that the intermittent state ($Q=5.78$)

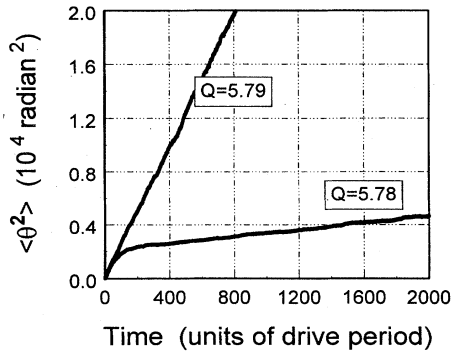

FIG. 10. Ensemble averages $\langle[\theta(\tau)]^2\rangle$ for the intermittent case $Q=5.78$ and for the neighboring chaotic case $Q=5.79$.

diffuses approximately 20 times more slowly than the purely chaotic state ($Q=5.79$).

An explanation for this observation can be found in the following argument. The two periodic modes, as has been mentioned, are nonrotating. Hence, during residence in either period-2 state, there is no diffusion whatever. In fact it is only during the chaotic bursts that diffusion can occur, and that diffusion will proceed at a rate very nearly equal to the slope of the $Q=5.79$ characteristic. In other words, the intervals spent on the periodic attractors can be thought of as "dead time" when diffusion is temporarily halted, while motion on the strange attractor is "active time." Suppose that η represents the average ratio of dead time to active time. Then diffusion will proceed only during the portion $1/(1+\eta)$ of any total observation time and will be "interrupted" for the portion $\eta/(1+\eta)$. From the point of view of a Poincaré section such as Fig. 9, η would be the ratio of the number of points contained in the attractor boxes to the number of points on the strange attractor external to the boxes. Data derived from a simulation run lasting for 8×10^5 drive cycles yielded $\eta=(762288)/(36713)=20.7$. Expressed another way, the system spends about 95% of the time on one or the other periodic attractor, and only 5% of the time moving between these attractors. This numerical value of η is in good agreement with the value obtained from slopes in Fig. 10.

We emphasize that our model for interrupted diffusion as an explanation for phase expansion during intermittent chaos retains the fundamental notion that diffusion, when it happens, follows the conventional law $\langle\theta^2\rangle\propto t$.

Finally, we turn to the issue of anomalous diffusion, which has attracted considerable interest recently [12–18]. The iterated maps in these studies exhibited mean-squared displacements that varied as t^γ when the systems were intermittently chaotic. In contrast, our results show normal deterministic diffusion ($\gamma=1$) for purely chaotic states, interrupted diffusion ($\gamma=1$) for intermittent chaos, and drift expansion ($\gamma=2$) in rotating periodic states. We think it significant, for example, that Geisel and Nierwetberg [4] report anomalous diffusion ($\gamma=2$) *only below* what they term a crossover time T_m. Above T_m they find conventional diffusion. So the ultimate expansion is always a standard diffusion, and the early anomalous behavior is perhaps strongly dependent on initial conditions—as we have seen in our results.

ACKNOWLEDGMENTS

Financial support was provided by a grant from the Natural Sciences and Engineering Research Council of Canada and by the WLU Office of Research. Parts of this work were performed under the auspices of the U.S. Department of Energy.

[1] G.L. Baker and J.P. Gollub, *Chaotic Dynamics: An Introduction* (Cambridge University Press, New York, 1990).
[2] M. Schell, S. Fraser, and R. Kapral, Phys. Rev. A **26**, 504 (1982).
[3] T. Geisel and J. Nierwetberg, Phys. Rev. Lett. **48**, 7 (1982).
[4] T. Geisel and J. Nierwetberg, Z. Phys. B **56**, 59 (1984).
[5] P. Reimann, Phys. Rev. E **50**, 727 (1994).
[6] R. Artuso, Phys. Lett. A **160**, 528 (1991).
[7] S. Prakash, C-K. Peng, and P. Alstrøm, Phys. Rev. A **43**, 6564 (1991).
[8] H. Fujisaka and S. Grossmann, Z. Phys. B **48**, 261 (1982).
[9] S. Grossmann and H. Fujisaka, Phys. Rev. A **26**, 1779 (1982).
[10] T. Geisel, A. Zacherl, and G. Radons, Z. Phys. B **71**, 117 (1988).
[11] S. Yanagida, H. Fujisaka, and M. Inoue, Prog. Theor. Phys. **87**, 1087 (1992).
[12] G. Zumofen and J. Klafter, Phys. Rev. E **47**, 851 (1993).
[13] G. Zumofen, J. Klafter, and A. Blumen, Phys. Rev. E **47**, 2183 (1993).
[14] J. Klafter, G. Zumofen, and M.F. Shlesinger, Physica A **200**, 222 (1993).
[15] G. Zumofen and J. Klafter, Physica D **69**, 436 (1993).
[16] R.N. Mantegna, J. Stat. Phys. **70**, 721 (1993).
[17] X-J. Wang and C-K. Hu, Phys. Rev. E **48**, 728 (1993).
[18] R. Bettin, R. Mannella, B.J. West, and P. Grigolini, Phys. Rev. D **51**, 212 (1995).
[19] D.G. Aronson, M.A. Chory, G.R. Hall, and R.P. McGehee, Comm. Math. Phys. **83**, 303 (1982).
[20] B.A. Huberman, J.P. Crutchfield, and N.H. Packard, Appl. Phys. Lett. **37**, 750 (1980).
[21] R.L. Kautz and J.C. Macfarlane, Phys. Rev. A **33**, 498 (1986).
[22] M. Octavio, Phys. Rev. B **29**, 1231 (1984).
[23] J.A. Blackburn, Z-J. Yang, S. Vik, H.J.T. Smith, and M.A.H. Nerenberg, Physica **26D**, 385 (1987).
[24] J.A. Blackburn, S. Vik, B. Wu, and H.J.T. Smith, Rev. Sci. Instrum. **60**, 422 (1989).
[25] A.H. MacDonald and M. Plischke, Phys. Rev. B **27**, 201 (1983).
[26] S. Chaudhuri, G. Gangopadhyay, and D.S. Ray, Phys. Rev. E **47**, 311 (1993).